ADVANCED FUNCTIONAL MATERIALS
www.afm-journal.de

AgCuS: A Single Material Diode with Fast Switching Times

*Philipp Deng, Alfred Rabenbauer, Kathrin Vosseler, Janio Venturini, and Tom Nilges**

Pnp-switchable semiconductor materials are capable of switching their electronic properties from *p*- to *n*-type conduction. Observed in the handful of discovered compounds, this behavior is usually accompanied by a temperature-dependent phase transition. During this transition, the dynamical rearrangement of a certain substructure enables the change of the predominant charge carrier type. Considering the immense demand for compact and flexible electronic components, one possible approach is the construction of unconventional one-compound diodes using these pnp-switchable materials. In this study, pnp-switchable AgCuS is applied to realize a functional one-compound diode. AgCuS is accessible in large quantities as bulk material in a simple and short timeframe. Featuring an addressable pnp-switch at 364 K, this material is suitable for diode generation and usage in varied applications. The diode properties of AgCuS devices are reported and illustrate its reversibility and flexibility for diode operation. The material is fully characterized with regards to its electrical and thermal properties, as well as its diode performance. Properties of AgCuS are discussed in relation to the pnp-switchable material $Ag_{18}Cu_3Te_{11}Cl_3$, which is successfully used to fabricate the first one-compound diode operating close to room temperature.

1. Introduction

Diodes are basic building units which allow electrical current to pass in only one defined direction. They act as one-way switches and have become a prerequisite for almost every electronic device.[1–5] To achieve this behavior, *n*- and *p*-type semiconductors have to be combined to form a pn-junction. This could either be addressed by the combination of two different materials, or at least by the defined creation of different doping levels within the device. As the continuous downscaling of diodes and transistors becomes more challenging, alternative designs for the construction of these electronic components are required.[6] One approach is the realization of a diode using one single material that can switch between *p*- and *n*-type depending on its temperature and phase.[7]

The first pnp-switchable material, $Ag_{10}Te_4Br_3$, was discovered in 2009. During heating, the material undergoes an order-disorder phase transition at 390 K, while at the same time a charge density wave (CDW) is created through the chain-like polytelluride substructure. This CDW results in the creation of mobile electrons, changing the predominant charge carrier type during the transition and therefore switching the semiconductor from *p*- to *n*-type conducting.[7]

In principle, this pn-switch without any external doping of the compound is an intriguing property, which was never observed before in an inorganic material. Via substitution in the anion and cation substructures this pn-switching effect was shifted in temperature in a range of 400 to 380 K.[8–10] Upon halide-substitution the pn-effect remains unchanged in $Ag_{10}Te_4Br_3$ while any chalcogenide-substitution hinders a CDW formation and therefore the pn-switch. This discovery led to an intensive search for additional compounds capable to perform such kind of electronic structure manipulations. In principle, a reversible and addressable pn-switch can be used to fabricate diodes and transistors if the *p*- and *n*-type conduction can be controlled in an easy way, the creation of *p*- and *n*-areas are defined, and the electronic structure variation leads to a defined electronic response. For these purposes the pn-switch needs to be located in a suitable temperature range, e.g. close to room or application temperature, and the diode formation needs to be reliable and controllable.

In the following years, three other inorganic compounds were identified which perform a pn-switch. $AgBiSe_2$ shows this pn-switch at 580 K, $Tl_2Ag_{12}Se_7$ at 410 K, and finally AgCuS at 364 K.[11–13] Evidently, the pn-transition temperature was lowered toward room temperature, where most devices and processes with diode or transistor contribution take place. Finally, with $Ag_{18}Cu_3Te_{11}Cl_3$ the first material was reported recently to show a pn-switch at room temperature. Using $Ag_{18}Cu_3Te_{11}Cl_3$, the first one-compound diode device was prepared and the diode formation and performance for this system were reported.[14] Another interesting attempt to fabricate a diode via pn-junctions was the realization of an organic single molecule diode.[15] Here, weakly coupled π-systems with donor and acceptor units that are attached to a rod can result in a diode-like U/I curve at 30 K.

The combination of *p*- and *n*-type semiconductors is not only used in electrical engineering, but also plays a key role in

P. Deng, A. Rabenbauer, K. Vosseler, J. Venturini, T. Nilges
School of Natural Sciences (NAT)
Department of Chemistry
Synthesis and Characterization of Innovative Materials Group
Technical University of Munich
Lichtenbergstraße 4, 85748 Garching b. München, Germany
E-mail: tom.nilges@tum.de

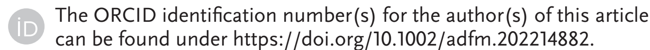
The ORCID identification number(s) for the author(s) of this article can be found under https://doi.org/10.1002/adfm.202214882.

© 2023 The Authors. Advanced Functional Materials published by Wiley-VCH GmbH. This is an open access article under the terms of the Creative Commons Attribution-NonCommercial License, which permits use, distribution and reproduction in any medium, provided the original work is properly cited and is not used for commercial purposes.

DOI: 10.1002/adfm.202214882

 © 2023 The Authors. Advanced Functional Materials published by Wiley-VCH GmbH

sensors, light emitting diodes (LEDs), catalytic processes and energy conversion system, e.g. solar cells, or thermoelectric devices.[3,16–24] In each of those processes, the pn-junction needs to be formed at a certain place (or *p*- and *n*-type semiconductors are separated in thermoelectric applications). As conventional diodes are non-volatile, the position of the junction or the semiconductors itself is not flexible and in principle defined by the doping type and level in a given material.

With the realization of one-compound diode devices, like in the case of $Ag_{18}Cu_3Te_{11}Cl_3$, it has been shown that a diode can be generated on demand and position-independently.[14] Once one-compound diodes are transferred into the aforementioned processes, this aspect may increase the flexibility of the device architecture drastically. With pnp-switching materials applied as one-compound diodes, more versatility can be achieved not only concerning the position, but in principle also in the direction of current flow. To realize a switch of the forward direction of the diode, only the temperature gradient has to be reversed in this one-compound diode device.

In this study we investigate the properties of AgCuS used as a one-compound diode. This mineral called stromeyerite was first characterized as a pnp-switchable material by Biswas et al.[13,25,26] They reported on the polymorphism, thermoelectric, electronic and pnp-switching properties of this intriguing material. Also the pnp-switching mechanism has been reported in this study. Reduction of particle size down to the nanometer regime and a certain non-stoichiometry in the Cu substructure ($AgCu_{1-x}S$, x = 0.01 to 0.04) resulted in a loss of the pn-switching property.[27,28] Defects in the silver substructure Ag_{1-x} CuS of up to 10% ($Ag_{1-x}CuS$, x = 0.01 to 0.15) are less critical and the pn-switch still takes place, but is less pronounced than in AgCuS.

2. Results and Discussion

2.1. Phase Analysis and Characterization of AgCuS

All pnp-switchable materials known until now – $Ag_{10}Te_4Br_3$, $Ag_{18}Cu_3Te_{11}Cl_3$, $Tl_2Ag_{12}Se_7$, $AgBiSe_2$, and the herein discussed AgCuS – show temperature dependent polymorphism.[7,11–14] The crucial role of those transitions concerning the semiconduction type is discussed in detail later on in this manuscript. For AgCuS, three different polymorphs are reported in the range of 298 to 439 K (see **Figure 1**).[13] Throughout those phase transitions, the cationic substructure becomes more and more disordered with increasing temperature. In the room temperature β-polymorph, crystallizing orthorhombically, in space group $Cmc2_1$ (36), Cu and Ag are completely ordered and therefore separated from each other on two different Wyckoff sites 4*a*. In the first high temperature α-phase, that is stable above 358 K (onset value determined from our own DSC experiments, with literature values 361[25] and 364 K[13]) and crystallizes hexagonally, in space group $P6_3/mmc$ (194), partial disorder in the cation substructure takes place and 25% of the copper atoms mix with silver atoms on partially occupied 12*k* sites. The rest of the copper atoms remains ordered on 2*b* sites. Upon further heating, the δ-polymorph is formed at 439 K, crystallizing cubically, in space group $Fm\bar{3}m$ (223). In this modification, the cations are completely disordered, resulting in a partial and mixed occupancy of Cu and Ag on 8*c* and 32*f* sites.[13,29] Representative structure sections including unit cells are depicted in Figure 1. Partial occupancy of sites is illustrated at the bottom part of Figure 1, bottom row, using open circles.

The powder XRD of our AgCuS sample synthesized via the method described by Biswas et al. is shown in **Figure 2**a.[13]

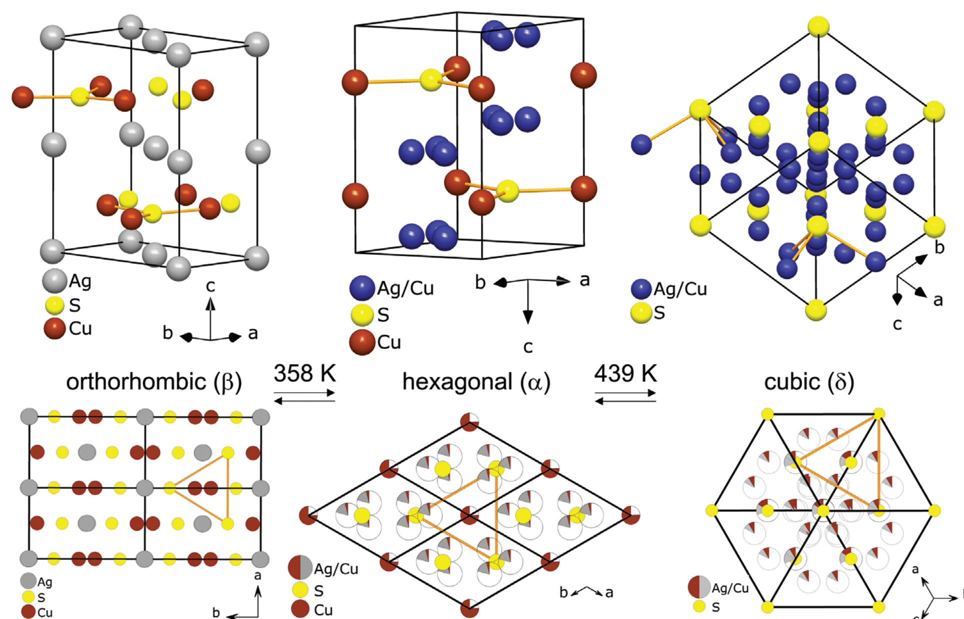

Figure 1. Top row: Selected structure motifs of the three different AgCuS polymorphs. Structure data taken from Biswas et al.[13] The different unit cells and a representative S-(Cu/Ag)$_3$ structure motif are displayed in the upper part. Bottom row: Changes in occupancy factors in the cation substructure. S_3 triangles are depicted in each polymorph to illustrate the changes in the crystal structure upon heating. A fully ordered cation substructure in the β-polymorph tends to disorder upon heating.

© 2023 The Authors. Advanced Functional Materials published by Wiley-VCH GmbH

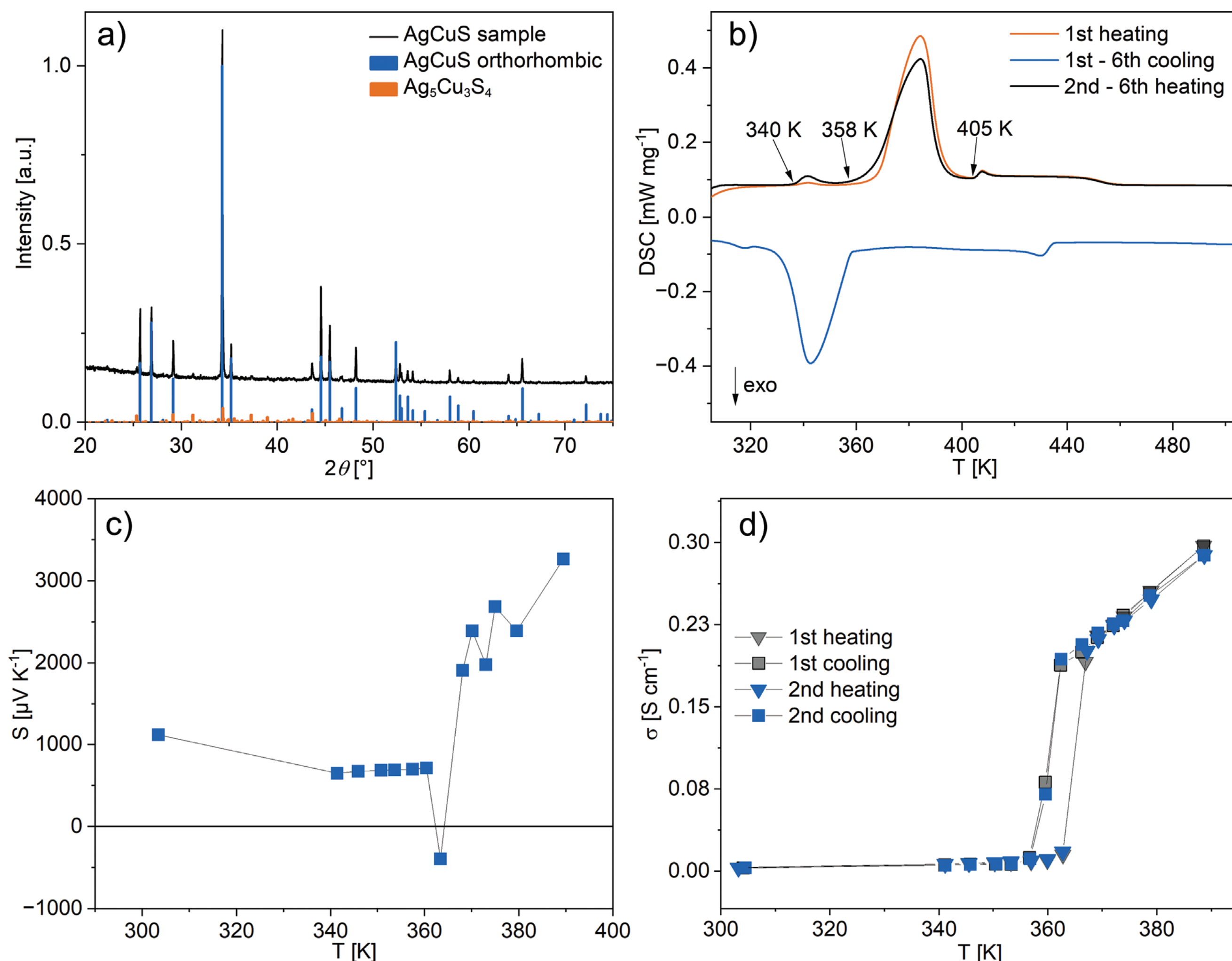

Figure 2. a) Powder XRD of the synthesized AgCuS sample, measured at 300 K. The theoretical patterns of AgCuS in the low-temperature orthorhombic phase (blue)[13] and $Ag_5Cu_3S_4$ (orange)[25] are depicted below. b) Differential scanning calorimetry curves of AgCuS sample for six consecutive cycles were measured. Two broad endothermal signals with onset points at 358 and 405 K are visible during first heating. An additional third very weak endothermal signal is already visible at an onset of 340 K which increases slightly in intensity in the second heating cycle. From 2nd to 6th cycle the thermal response is identical for heating and cooling. c) Seebeck coefficient measurement of AgCuS in a range of 303 to 388 K, displaying the pnp-switching ability of the material. d) Electrical conductivity measurement of AgCuS in a range of 303 to 388 K. Lines between the points are drawn to guide the eyes.

These reflections were indexed and refined using an orthorhombic symmetry, in the space group $Cmc2_1$, resulting in refined cell parameters of a = 7.974(5) Å, b = 6.627(4) Å, c = 4.066(2) Å, and V = 214.9(4) Å^3. These values are nearly identical to those reported in the CIF data for the mineral stromeyerite (a = 4.0673 Å, b = 6.6406 Å, c = 7.9711 Å, V = 215.3 Å^3).[25] AgCuS reflections (blue lines in Figure 2a) were calculated on the basis of the room temperature data reported herein.[25]

Besides the main phase, small impurities of the silver-rich phase $Ag_5Cu_3S_4$ can be recognized in the bulk material.[29] This phase was identified as the mineral mckinstryite, exhibiting a very similar crystal structure compared to stromeyerite in space group *Pnma*. The amount of the side phase was determined as 7% by a Rietveld refinement profile fit (see Figure S1, Supporting Information). No undefined reflections remained after identifying the two phases. EDX analysis resulted in a composition of 1.1(1):1.0(1):1.0(1) (Ag:Cu:S) for the main fraction AgCuS.

We compared our XRD data with the results from Biswas et al. and detected traces of our side phase in their temperature dependent AgCuS data, especially in their reported 333 K cooling sample.[13] After this detailed phase analysis of our AgCuS sample it can be concluded that the product is sufficiently pure to create a single-material diode device.

In order to verify the thermal stability of AgCuS prior to our diode measurements we performed several heating and cooling cycles between room temperature and 500 K. Data from differential scanning calorimetry (DSC) experiments for six consecutive cycles are denoted in Figure 2b. Cycles 2 to 6 are fully identical and therefore only the 2nd cycle is plotted.

The DSC measurement shows one very intense endothermal signal at 358(1) K (onset value) in the heating cycle, representing the AgCuS transition from the orthorhombic room temperature β-polymorph to the hexagonal α-phase, which also represents the pn-switching transition. Between 405 and

© 2023 The Authors. Advanced Functional Materials published by Wiley-VCH GmbH

440 K the thermal effect related to the α-δ transition takes place, when further disordering of the cations occurs. Upon cooling, an effect occurs at 433(2) K, marking the temperature at which the cations are again locked into the more ordered hexagonal phase. Those results exactly match the findings in the first heating cycle reported by Biswas et al. (see Supporting Information).[13] The authors also described the additional signal at ≈408 K associated to the low-temperature boundary of the two-phase hexagonal-cubic region.

In our study, we find an additional broad endothermic effect at 350(2) K (peak maximum), which gains intensity from the first to the second heating cycle but remains constant in the third one. In the cooling curve a related broad exothermic effect is visible at ≈320(2) K. The DSC curve of Biswas et al. shows a similar exothermic effect in their cooling cycles, but this one is not explicitly explained in their study.[13] Since an impurity of the silver-rich phase $Ag_5Cu_3S_4$ is identified by P-XRD, one might expect this side phase to create the two effects. Therefore, we synthesized a phase pure sample of $Ag_5Cu_3S_4$ in the same way as AgCuS and measured a DSC curve for the pure material. $Ag_5Cu_3S_4$ exhibits a phase transition at 369(1) K (onset value), and 407(1) K (onset value) (see Figure S2, Supporting Information). It is therefore most likely that the additional effects and the 408 K effect mentioned before are caused by $Ag_5Cu_3S_4$ or possibly by another non-crystalline phase. A secondary process during the final ordering in the cation substructure is also possible.

For the utilization of such a pn-switchable material as a one-compound diode, *p*- and *n*-type regions have to be created in the device simultaneously. To initiate this feature, a temperature gradient is a suitable method to generate both regions in a single crystal just by inducing the β-α phase transition from the *p*-type before and above the transition to the *n*-type conducting transition stage at the phase transition itself. Our group recently showed for the first time the feasibility of such a process using another pn-switchable material, $Ag_{18}Cu_3Te_{11}Cl_3$, in which a phase transition ≈296 K is used to create both semiconductor types and therefore a one-compound diode out of only one material.[14]

We compared the enthalpy of the two pnp phase transitions, of $Ag_{18}Cu_3Te_{11}Cl_3$ at 296 K, with the one of AgCuS at 358 K (see Figure S3, Supporting Information) and found only a very small transition enthalpy of 0.2 J g^{-1} for $Ag_{18}Cu_3Te_{11}Cl_3$ in contrast to 31.1 J g^{-1} for AgCuS.

The phase transition in $Ag_{18}Cu_3Te_{11}Cl_3$ is purely of second order, as no significant cell volume or property jump was reported in $Ag_{18}Cu_3Te_{11}Cl_3$. The *n*-type conduction occurs after the structural phase transition and is initiated by a partial disorder of Te atoms in the anionic substructure, accompanied by the creation of a partial 2D CDW. Neither a change in the space group nor a significant cell volume jump occurs during this β-α $Ag_{18}Cu_3Te_{11}Cl_3$ phase transition. Therefore, the amount of consumed heat is relatively low and the resulting endothermic DSC signal during heating is small. Evidently, AgCuS needs a larger amount of energy for a successful rearrangement or displacement of the cations during the pnp-switching β-α phase transition.

The pnp-switch itself was substantiated by Seebeck coefficient measurements for AgCuS. As illustrated in Figure 2c the Seebeck coefficient changes its sign during the β-α phase transition. Between room temperature and up to 360 K, coefficients range from +648 to +1122 µV K^{-1} while a drop to −393 µV K^{-1} occurs at 363 K. At slightly higher temperatures the sign of the Seebeck coefficient is again switched to high positive values. This effect is reversible and has been observed in consecutive measurement cycles as illustrated in Figure S5 (Supporting Information).

During this β-α transition, we also observed a significant change in the electrical conductivity. The evolution of the temperature-dependent electrical conductivity measurement of a bulk AgCuS ingot is displayed in Figure 2d. At up to 363 K, only a small rise in conductivity from 3 to 10 mS cm^{-1} is visible with increasing temperature. Between 363 and 366 K, the conductivity suddenly rises to 0.2 S cm^{-1}and increases linearly up to 0.3 S cm^{-1} at 387 K. This jump occurs right at the β-α phase transition, enabling higher total electrical conductivities. It is most likely that the emerging cation disorder causes this phenomenon because of the enhanced cation mobility. In general, the increase in conductivity with temperature perfectly displays the behavior of a semiconducting material, and the determined values are in the same region reported by Biswas et al.. The only difference to the findings of Biswas et al. is that our samples do not show a significant conductivity increase at the phase transition temperature itself, which could have occurred due to the fact that we simply did not measure it within our temperature steps (see Figure S4, Supporting Information).

We therefore classify this β-α phase transition of mixed order with a significant first order contribution. The question of whether this first order contribution will affect the diode formation and performance will be addressed in the following part. It is not the purpose of this study to redetermine the pnp-switching mechanism. This mechanism was reported and perfectly described by Biswas et al. in their outstanding manuscript.[13] The interested reader is asked to refer to the original literature or the supplement section where a brief summary of the underlying mechanism is given. All experiments reported so far were performed to evaluate the quality of AgCuS prior to the diode measurements and to verify the successful occurrence of the pnp-switch.

2.2. AgCuS Diode Fabrication and Performance

Crystals of AgCuS were mounted onto printed circuit boards (PCB), as shown in **Figure 3**a. Tin/lead solder was used as contact medium. The heating elements (56 Ω resistors) next to one contact can be activated independently from those on the other side, allowing for the creation of a thermal gradient in the device. If a current is applied to the paired resistors, heat is generated locally. The thermal gradient during this state was analyzed with a Micro-IR camera; the resulting image can be seen in Figure 3b. During this stage, the crystal is submitted to a temperature gradient of 333 to 368 K at the cold and hot contacts, respectively.

The electrical behavior of the produced device was characterized at two different temperature conditions, isothermally at a given temperature and operated within a certain temperature gradient.

© 2023 The Authors. Advanced Functional Materials published by Wiley-VCH GmbH

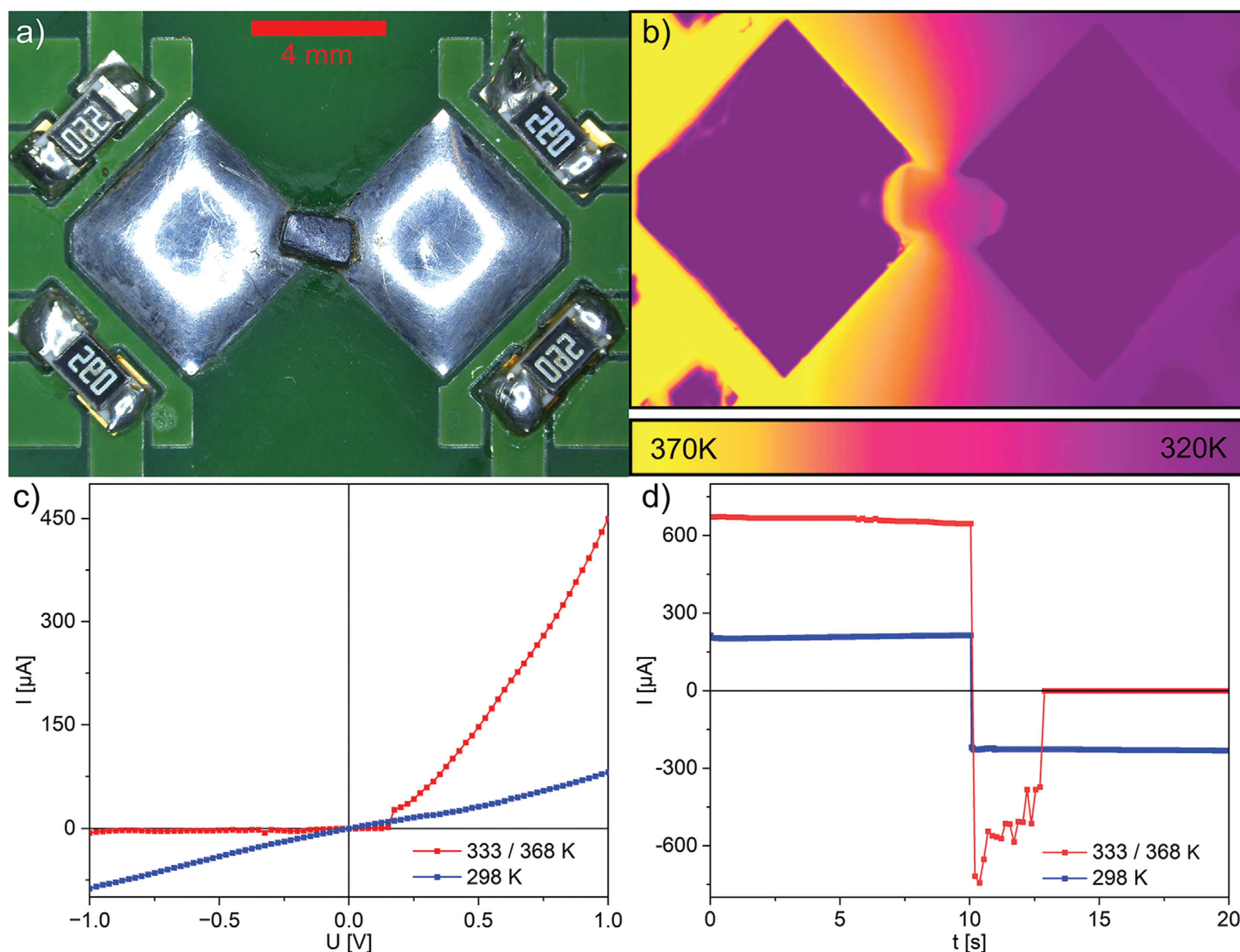

Figure 3. a) Optical microscope image of an AgCuS sample mounted onto a PCB. The contacts are produced with the aid of tin/lead solder to provide ohmic behavior between the gold pads and the crystal. Two 56 Ω resistances per contact are used to specifically heat up alternating sides of the crystal to induce pn-regions across it. b) Thermal image of the device in a 333 to 368 K temperature gradient. c) UI curves of the PCB-mounted crystal at 298 K (blue) and with a gradient of 333 to 368 K (red). d) Switching time of the produced devices under isothermal conditions (298 K) and with the application of a 333/398 K gradient. A potential of 1.0 V was applied to the device up to t = 10 s, after which the signal of the potential was inverted.

With the resistances turned off, the entire system operates isothermally at 298 K. The U/I curve measured between ±1 V under these circumstances is that of a non-rectifying element, with a symmetrical character regardless of the applied potential. As shown in Figure 3c the isothermal conditions lead to the behavior expected of a regular resistive semiconductor with good ohmic contact, indistinguishable from a perfect resistance (blue curve). The linear dependence between potential and current also rules out the formation of a Schottky diode with the metallic contacts.

The second measurement condition includes the application of heat to the system via resistivity heating. Due to our experimental setup conditions the gradient starts at 320 K at the cold end. Evidently, room temperature would also work in this case. The system is thus led to the state described in Figure 3b, with a thermal gradient of 333/368 K through the crystal, encompassing both the *p*- and *n*-type regions of AgCuS. The heat dissipation is tuned in such a way that the β-α phase transition temperature and therefore also a pn-junction is localized exactly within the mounted crystal. This results in a region where electrons are the majority charge carriers (*n*-type) on the hot side, while at the colder side the conductivity is dominated by holes (*p*-type). At a certain position between these regions, the created temperature profile should thus lead to the formation of a pn-junction. This new region is called ambijunction,[14] to differ it from static pn-junctions formed by doped semiconductors.

The U/I curve of the system under these conditions is dramatically different, as denoted in Figure 3c (red curve). A classical diode behavior is observed, with a forward current 75 times higher than the reverse current at ±1 V. The rectifying character confirms the formation of a pn-ambijunction in this device. The junction potential was determined from different ingots resulting in values between 0.15 and 0.6 V, likely due to the slightly different ingot sizes or thermal conditions, with the consequent varying charge carrier density. In the following we illustrate results on one selected system with a 0.15 V junction potential. The forward current for the AgCuS diode of 450 µA is higher than that measured for $Ag_{18}Cu_3Te_{11}Cl_3$. Here the value

© 2023 The Authors. Advanced Functional Materials published by Wiley-VCH GmbH

is 140 µA. The power transmitted through the present AgCuS diode at +1 V in the forward direction is therefore four times higher than that of its previously mentioned counterpart.

In order to confirm the formation of a pn-ambijunction, the switching time of these systems was also measured at the two different temperature conditions (see Figure 3d). In this study, the systems were polarized with a forward potential (+1.0 V) for 10 s, after which a reverse potential of the same magnitude was applied and held. The isothermal curves at 298 K (blue curve in Figure 3d) show no evidence of current rectification. Currents of same magnitude but inverse direction were obtained after switching the polarization of the system, indicating a purely resistive behavior.

When the experiments were repeated with the application of the thermal gradient (red curve in Figure 3d), a classical diode response was observed. Initially, a relatively stable and intense current is measured due to the discharge of the excess minority charge carriers that were injected during the forward regime.

The linear removal of these excess carriers leads to a rather stable current, with a switching time t_s of 2.5 s. This aspect can be found between 10 and 12.5 s in Figure 3d. At $t > t_s$, where the fall time regime t_f supposedly starts, the reverse current usually decays exponentially toward the saturation current of the diode. In the present case, the fall time t_f is faster than the resolution of our measurement setup, thus it could not be measured precisely. We only observed a sudden decrease of the current. Almost immediately after the linear phase, the AgCuS diode shuts off and current is mostly blocked from traveling through the device.

The total time involved with the switching of this diode is much faster than the one previously reported for $Ag_{18}Cu_3Te_{11}Cl_3$. Diodes created with this compound are reported to shut current off after 62.4 s (t_s+t_f). On the other hand, AgCuS shows a much faster blocking speed, discharging excess charge carriers and creating a depletion region ≈25 times faster than its counterpart. The faster switching times could be associated to the different temperature regimes: while AgCuS shows the pnp-transition at ≈364 K, this phenomenon happens much closer to room temperature in $Ag_{18}Cu_3Te_{11}Cl_3$ (≈290 K). With more thermal energy, the charge carriers in AgCuS – both majority and minority – supposedly have increased mobility, diffusing much faster through the *p*- and *n*-regions and leading to faster switching times.

Moreover, the reversible formation and cancellation (or on- and off-switching) of a one-compound diode was analyzed in this study for the first time. The thermal gradient was consecutively introduced and removed from the system in order to analyze the reversibility and reliability of diode formation in these devices. **Figure 4** shows the U/I curves created after application of three consecutive heating cycles over the same device. A heating cycle represents the application of a temperature gradient (333 to 368 K) and the switch to an isothermal stage (298 K) afterward. An initial heating step leads to the production of the diode for the first time in this system. When the heat source is turned off and the temperature gradient decays, the rectifying behavior starts to falter, dying off completely once the crystal cools down beyond the temperature where the *n*-type material exists. If the heating elements are turned on again to reapply a temperature gradient, the system starts to show hints of rectification. A full diode is established once the thermal conditions are back to their optimized state and the needed temperature gradient is present (333 and 368 K at the cold and hot sides, respectively). This experiment was repeated three times, as illustrated in Figure 4. AgCuS can be tuned by an external

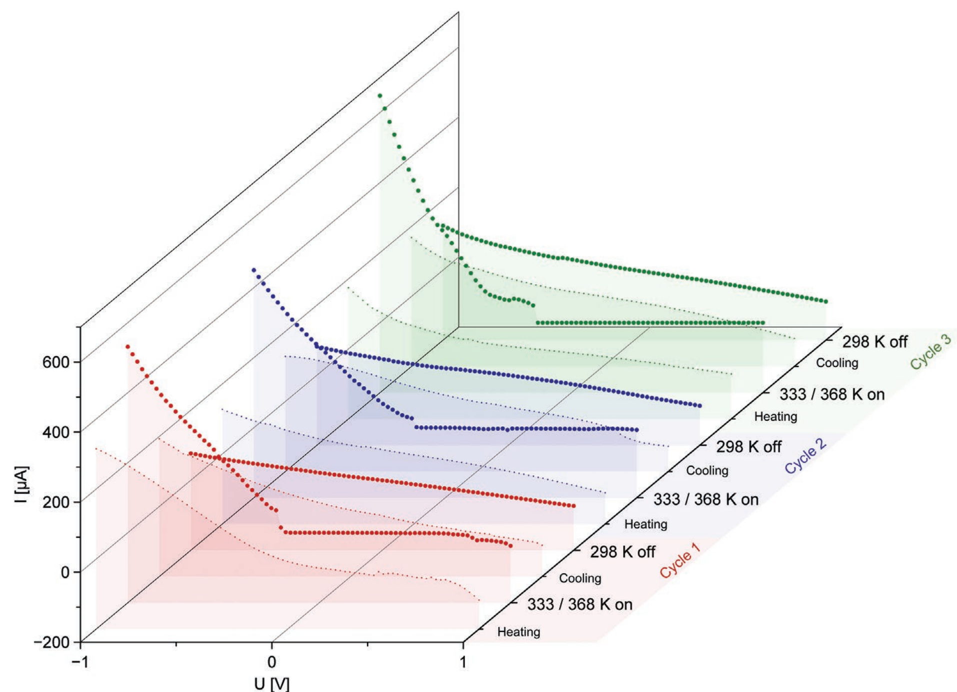

Figure 4. On/off-switching of the single-material diode. A thermal gradient was created and removed three consecutive times over the same device. The diode behavior is seen only when the *p*-and *n*-regions are present simultaneously.

 © 2023 The Authors. Advanced Functional Materials published by Wiley-VCH GmbH

temperature gradient and act as a one-compound diode where the diode formation and cancellation are fully reversible.

Certain differences in the U/I curves between Cycle 1 and Cycle 3, either in resistance or in the curve profile are most probably due to slight differences in the applied temperature gradient from measurement to measurement. It has to be stated that the measurements are performed against lab atmosphere and no shielding was applied to the PCB to avoid thermal convection. Since the temperature state in each of the cycles is not exactly the same and the *n*- or *p*-character is strongly dependent on temperature, the junction potential might also be affected, in the same manner it would if we changed the dopant concentration in a normal diode.

In Figure 2b one can observe a certain hysteresis in the DSC experiments between heating and cooling cycles during the pnp-switch phase transition. The formation of the diode was not affected by this hysteresis because we always illustrated the diode formation by heating of the system from room temperature to the transition temperature. The cancellation of the diode was not measured by us but it will take place once the T-gradient and therefore the pn-junction vanishes, most likely at slightly lower temperatures than for the formation.

Furthermore, this test showcases the flexible (volatile) diode formation potential of this new type of device. One-material diodes are very different from all other types of applied diodes in the sense that they are non-permanent. The rectifying diode behavior is only displayed if the system is operated under a certain temperature gradient. Otherwise, the same system displays a regular resistive character. When requested, AgCuS may block the passage of current in one direction, remaining virtually oblivious to any directionality in passage of charge under different circumstances.

An extra degree of freedom in the utilization of one-compound diode materials in devices or processes is the possibility of choosing the direction of current flow. In principle, the forward direction of a diode is defined once it is fabricated. With the present reversible one-compound diode devices, the forward direction of the diode can be adjusted by the orientation of the applied temperature gradient. To prove this feature, we reversed the applied temperature gradient and measured the electronic response afterward. A first diode was formed by heating the system on the right side, as shown in **Figure 5**a,c. The previously described rectifying behavior was observed. The heating elements were then turned off and the system was cooled down to room temperature (Figure 5b). The linear U/I response of a resistance was measured, indicating that the initial diode was annihilated. Subsequently, after reversing the temperature gradient, a diode was again produced, but with a forward direction

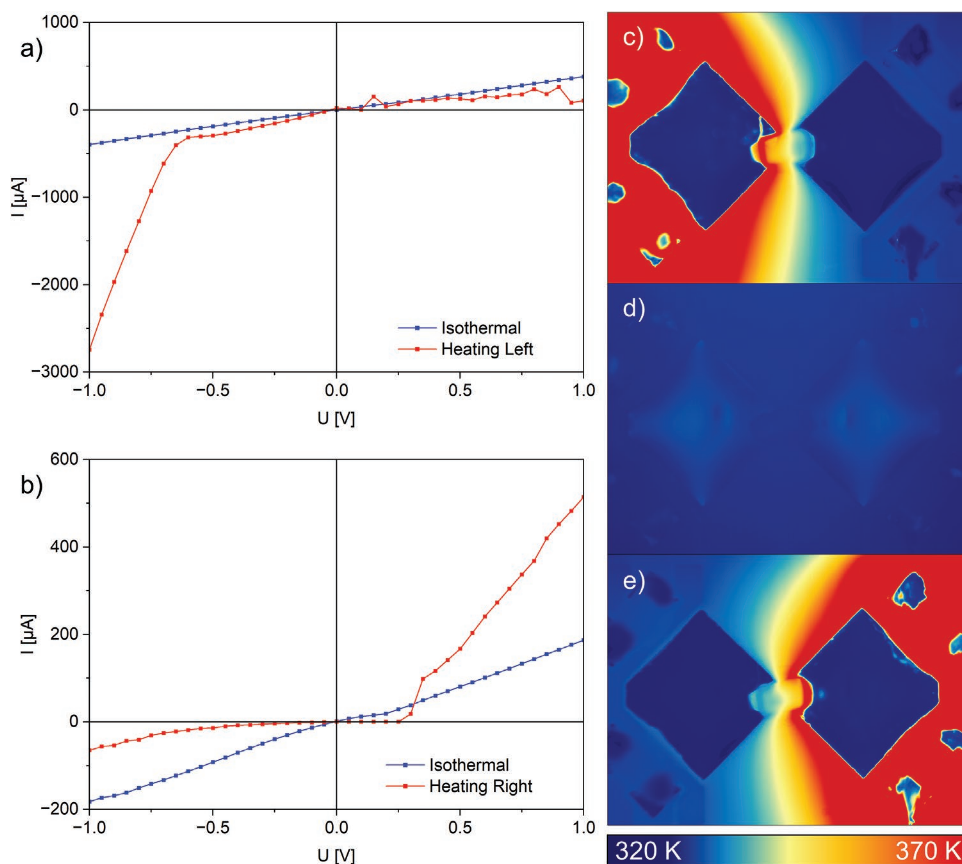

Figure 5. The forward direction of the diodes can be switched by alternating the direction of the heat gradient (a and b). When the left side is heated, the diode is blocking for positive voltages a). When the right side is heated, the diode is blocking for negative voltages b). The dissipation of the heat within the crystal was visualized via infrared imaging. With resistivity heating, the PCB and therefore the crystal can be independently heated at the left side c) or right side e). No temperature gradient is visible across the crystal under isothermal conditions at room temperature d).

© 2023 The Authors. Advanced Functional Materials published by Wiley-VCH GmbH

opposite to that in the previous case, see Figure 5b,e. As the position of the *p*- and *n*-regions was reversed, the direction of the forward current was also inverted, and current is now allowed to pass only in the direction opposite to that of the previous configuration.

Differences in total current and junction potential are accounted by different temperature conditions and contact areas on the two sides of the crystal. The total time for this experiment was of ≈15 min, which was the time associated with the establishment of a stable thermal gradient; once the gradient is present, the diode behavior is displayed virtually instantaneously.

3. Discussion

In this study, two new processes for diodes are illustrated for the first time, a) the reversible on- and off-switching of a diode by a one-compound pnp-material via a temperature gradient (and without doping), and b) the variable definition of the forward direction of a diode by a simple modification of the temperature gradient orientation.

In state-of-the-art diodes, a) is not possible and b) could only be mimicked by manually reconnecting the diode contacts. After manufacturing of integrated circuits, this direction switch is virtually impossible without strenuous manipulation. In the case of our devices, the blocking direction can be chosen by tweaking the temperature gradient that is applied to the system. Careful thermal control thus also allows the definition of the direction in which these novel devices conduct current, and likewise the direction through which no transport is allowed.

The processes a) and b) are unique in regular semiconducting devices. Diodes created via pnp-switching compounds can be formed selectively at a position where they are needed. Commonly used diodes present switching in either forward or blocking modes in a pre-defined direction. One-material diodes allow the selection of the forward direction in devices by the simple application of an external temperature gradient. This unique feature allows completely new architectures for diode devices and generates alternative pathways for applications of diodes in different processes. On top of this extra degree of freedom, the described devices show another further switch, between pn and np characters. With the standard thermal gradient, the system has a specific forward direction. With the symmetric reversion of the thermal gradient through the device, the forward direction is also inverted, meaning that current can now be transmitted only in the opposite orientation.

A certain drawback of AgCuS seems to be the operation temperature needed for the pnp-switch which is ≈363 K, in relation to the switching temperature of $Ag_{18}Cu_3Te_{11}Cl_3$ at room temperature. Due to the very low thermal conductivity of 0.5–0.7 W m^{-1} K^{-1} (data taken from[13]) an external temperature pulse might be applied locally without a strong heat dissipation in the system. Therefore, the slightly higher T-gradient, or better, the high T-value of the gradient needed in AgCuS might be more energy consuming to generate but it also accelerates the necessary ion displacement and diffusion during the phase transition process.

4. Conclusion

The composition, polymorphism, and semiconducting properties of AgCuS were re-assessed in order to confirm the quality of AgCuS as pnp-switching compound and therefore its suitability for creating a single-material diode. In this work, AgCuS ingots were successfully used to create a one-compound diode and determine its switching abilities.

A stable diode could be created, outperforming $Ag_{18}Cu_3Te_{11}Cl_3$, the first reported one-compound diode material, in terms of switching time and forward current. Due to the pn-transition temperature of 364 K ensuring a certain thermal distance to ambient conditions, the formation and maintenance of the pn junction is easy to realize in practice. Furthermore, the orientation of the forward direction of the diode can be adjusted by selecting a suitable thermal gradient, which is not possible for classical diodes. Those findings not only substantiate the creation of position- and current direction-independent diodes, but also enable the usage of one-compound diode materials in electrocatalysis, photocatalysis, or energy conversion processes, where an already present temperature gradient could be utilized to create diodes locally. In a next step, we intend to fabricate flexible transistors, further pushing the opportunities toward single-material electronic devices.

5. Experimental Section

Synthesis of AgCuS: AgCuS was synthesized as described by Biswas et al.[13] The material was prepared by a melting reaction directly from the elements using silver (Chempur, 99.999%), copper (Chempur, 99.999%), and sulphur (Alfa Aesar, 99.999%) on a 7 g scale. Stoichiometric amounts of the starting materials were sealed into evacuated silica glass ampules and heated slowly to 773 K for 12 h. Afterward the temperature was increased to 1223 K in 5 h and held for 24 h. The material was then quenched by quick removal of the ampoule from the oven and exposure to air. Small amounts of silver residue on the surface were removed by polishing, leading to black shiny ingots of AgCuS. The product was cut into mm-sized pieces prior to use.

Powder X-ray Diffraction (P-XRD): For phase analysis, small amounts of finely ground sample were placed between two stripes of Scotch Magic Tape. Powder XRD data was collected in the range of 5.00 to 79.09 2θ with a Stoe STADI P powder diffractometer equipped with a position sensitive Dectris Mythen 1K detector using Cu $K_{\alpha 1}$ radiation (λ = 1.54060 Å, curved Ge(111) monochromator). Phase analysis was carried out using the Stoe WinXpow software package.[30]

Thermal Analysis: A small piece of the ingot was transferred to an aluminum crucible under inert conditions and differential scanning calorimetry was performed with a Netzsch DSC 200 F3 Maia device. The measurement was conducted under N_2 atmosphere in the temperature range of 298 to 523 K with a heating/cooling rate of 10 K min^{-1}. Thermal effects were derived from onset temperatures when possible. Data analysis was performed using the Netzsch Proteus Thermal Analysis software package.[31]

Semi-quantitative Phase Analyses and Scanning Electron Microscopy (SEM): The samples were fixed on a steel holder with a conductive adhesive polymer tape from Plano GmbH. Energy dispersive X-ray spectroscopy (EDX) was performed using a Jeol JSM-IT200 InTouchScope™ with an integrated Jeol JED-2300 EDX unit. The acceleration voltage was set to 10 kV. The EDX results were averaged from at least three different points, selected randomly on the crystal surface. An error of 10% was estimated for all composition values.

Thermal Imaging via a Microbolometer-based Camera: Thermal images were collected by a Infratec VarioCam HD head 980 S microbolometer

© 2023 The Authors. Advanced Functional Materials published by Wiley-VCH GmbH

system equipped with a Jenoptik M = 1.0× precision microscopy objective. The images were processed with the Irbis 3.1 professional software package.[32] Pictures were acquired with activated microscan unit resulting in a nominal resolution of 2048 × 1536 pixel. Temperature accuracy at 303 K +/−1.5 °C, thermal resolution 0.03 K.

Measurements of Electrical Conductivity and Seebeck Coefficient: An as-prepared AgCuS ingot was cut into a bar of ≈14 × 10 × 3 mm. The Seebeck coefficient and the electric conductivity were measured simultaneously directly with a Netzsch SBA 458 Nemesis under a continuous argon flow. The electrical conductivity was determined using a four-point probe measurement. The technical measurement error was ±7% for the Seebeck coefficient and ±5% for the electrical conductivity. Data analysis was performed with the Netzsch SBA-measurement software package.[33]

Diode Characterization: A cut sample of the AgCuS ingot was mounted onto a printed circuit board (PCB) by soldering it onto the gold-plated contacts with a tin/lead solder (Stannol, composition Sn:Pb:Cu = 60:39:1 wt.%), see Figure 3a. For the application of directional heat gradients, a pair of 56 Ω resistances was placed next to each of the contacts. Those were used to independently heat up the contacts and therefore create a heat gradient through the ingot. A QJE PS6005 switching power supply was used to provide the electrical current for the resistive heating. For AgCuS, the measurements could be conducted at ambient conditions, since the β-phase was prominent up to 369 K. For the diode measurements, a heat gradient from 338 to 363 K was applied to the ingot. Temperature was controlled by an external thermocouple (RSpro thermometer device, Ni/Cr/Ni type thermocouple, accuracy ±1 K) at the contacts during the measurements as well as by the aforementioned thermal imaging device. Conductivity measurements were performed using a Keithley 2450 SourceMeter®. Voltage errors are ±0.015% and current errors are ±0.03%. This digital multimeter was operated with the aid of KickStart I-V Characterizer App. Measurements were performed at a scanning speed of 0.06 V s^{-1}. Data analysis was performed with the Keithley Kickstart IV Characterizer App software package.[34]

Supporting Information

Supporting Information is available from the Wiley Online Library or from the author.

Acknowledgements

P.D. and A.R. contributed equally to this work. K.V. conducted the SEM and EDX measurements. P.D., A.R., J.V., and T.N. wrote the manuscript. A.R., P.D., and K.V. thank the TUM Graduate School for support. J.V. thanks for a stipend funded by the TUM Talent factory program. This project was supported in part by the international graduate school ATUMS, IRTG 2020 funded by the German Science Foundation DFG, and by the DFG Grant NI1095/12.

Open access funding enabled and organized by Projekt DEAL.

Conflict of Interest

The authors declare no conflict of interest.

Data Availability Statement

The data that support the findings of this study are available from the corresponding author upon reasonable request.

Keywords

ambijunctions, ion conductors, one-compound diodes, pnp-switching, semiconductors

Received: December 21, 2022
Revised: January 17, 2023
Published online: February 20, 2023

[1] J.-P. Colinge, C. A. Colinge, *Physics of semiconductor devices*, Springer, NY, USA **2006**.
[2] U. V. Ghorpade, M. P. Suryawanshi, M. A. Green, T. Wu, X. Hao, K. M. Ryan, *Chem. Rev.* **2022**.
[3] L. Heng, X. Wang, N. Yang, J. Zhai, M. Wan, L. Jiang, *Adv. Funct. Mater.* **2010**, *20*, 266.
[4] K. Potje-Kamloth, *Chem. Rev.* **2008**, *108*, 367.
[5] M. Y. Wong, C. Y. Tso, T. C. Ho, H. H. Lee, *Int. J. Heat Mass Transfer* **2021**, *164*, 120607.
[6] J. P. Sun, G. I. Haddad, P. Mazumder, J. N. Schulman, *Proc. IEEE* **1998**, *86*, 641.
[7] T. Nilges, S. Lange, M. Bawohl, J. M. Deckwart, M. Janssen, H.-D. Wiemhöfer, R. Decourt, B. Chevalier, J. Vannahme, H. Eckert, R. Weihrich, *Nat. Mater.* **2009**, *8*, 101.
[8] T. Nilges, M. Bawohl, *Z. Naturforsch., B: Chem. Sci.* **2008**, *63*, 629.
[9] T. Nilges, M. Bawohl, S. Lange, *Z. Naturforsch., B: Chem. Sci.* **2007**, *62*, 955.
[10] O. Osters, M. Bawohl, J.-L. Bobet, B. Chevalier, R. Decourt, T. Nilges, *Solid State Sci.* **2011**, *13*, 944.
[11] C. Xiao, X. Qin, J. Zhang, R. An, J. Xu, K. Li, B. Cao, J. Yang, B. Ye, Y. Xie, *J. Am. Chem. Soc.* **2012**, *134*, 18460.
[12] Y. Shi, A. Assoud, C. R. Sankar, H. Kleinke, *Chem. Mater.* **2017**, *29*, 9565.
[13] S. N. Guin, J. Pan, A. Bhowmik, D. Sanyal, U. V. Waghmare, K. Biswas, *J. Am. Chem. Soc.* **2014**, *136*, 12712.
[14] A. Vogel, A. Rabenbauer, P. Deng, R. Steib, T. Böger, W. G. Zeier, R. Siegel, J. Senker, D. Daisenberger, K. Nisi, A. W. Holleitner, J. Venturini, T. Nilges, *Adv. Mater.* **2022**, 2208698, https://doi.org/10.1002/adma.202208698.
[15] M. Elbing, R. Ochs, M. Koentopp, M. Fischer, C. von Hänisch, F. Weigend, F. Evers, H. B. Weber, M. Mayor, *Proc. Natl. Acad. Sci. USA* **2005**, *102*, 8815.
[16] C. Dai, Y. Liu, D. Wei, *Chem. Rev.* **2022**, *122*, 10319.
[17] M.-H. Fang, Z. Bao, W.-T. Huang, R.-S. Liu, *Chem. Rev.* **2022**, *122*, 11474.
[18] J. Briscoe, M. Stewart, M. Vopson, M. Cain, P. M. Weaver, S. Dunn, *Adv. Energy Mater.* **2012**, *2*, 1261.
[19] S. Hadke, M. Huang, C. Chen, Y. F. Tay, S. Chen, J. Tang, L. Wong, *Chem. Rev.* **2022**, *122*, 10170.
[20] K. He, T. Tadesse Tsega, X. Liu, J. Zai, X.-H. Li, X. Liu, W. Li, N. Ali, X. Qian, *Angew. Chem., Int. Ed.* **2019**, *58*, 11903.
[21] R. He, G. Schierning, K. Nielsch, *Adv. Mater. Technol.* **2018**, *3*, 1700256.
[22] H. Li, C. Chen, Y. Yan, T. Yan, C. Cheng, D. Sun, L. Zhang, *Adv. Mater.* **2021**, *33*, 2105067.
[23] P. V. Pham, S. C. Bodepudi, K. Shehzad, Y. Liu, Y. Xu, B. Yu, X. Duan, *Chem. Rev.* **2022**, *122*, 6514.
[24] X.-L. Shi, J. Zou, Z.-G. Chen, *Chem. Rev.* **2020**, *120*, 7399.
[25] D. Santamaria-Perez, A. Morales-Garcia, D. Martinez-Garcia, B. Garcia-Domene, C. Mühle, M. Jansen, *Inorg. Chem.* **2013**, *52*, 355.
[26] D. M. Trots, A. Senyshyn, D. A. Mikhailova, M. Knapp, C. Baehtz, M. Hoelzel, H. Fuess, *J. Phys.: Condens. Matter* **2007**, *19*, 136204.

© 2023 The Authors. Advanced Functional Materials published by Wiley-VCH GmbH

[27] M. Dutta, D. Sanyal, K. Biswas, *Inorg. Chem.* **2018**, *57*, 7481.
[28] S. N. Guin, D. Sanyal, K. Biswas, *Chem. Sci.* **2016**, *7*, 534.
[29] U. Kolitsch, *Mineral. Mag.* **2010**, *74*, 73.
[30] Stoe, *WinXPOW*, version 3.05, Stoe & Cie GmbH Darmstadt, Germany **2011**.
[31] Netzsch. GmbH, *Proteus Thermal Analysis*, version 5.2.0, Netzsch Gerätebau GmbH, Selb, Germany **2010**.
[32] InfraTec., *IRBIS 3.1 professional*, version 3.1.114, InfraTec GmbH, Dresden, Germany **2022**.
[33] Netzsch. GmbH, *Netzsch S. B. A.-M.*, version 2.0.7.0, Netzsch Gerätebau GmbH, Selb, Germany **2016**.
[34] Keithley Instruments LLC, *Kickstart IV Characterizer App*, version 2.5.0, Tektronix Inc., Beaverton, USA **2021**.
[35] https://creativecommons.org/licenses/by/3.0/

© 2023 The Authors. Advanced Functional Materials published by Wiley-VCH GmbH